Materials and Design 96 (2016) 283–295

Contents lists available at ScienceDirect

Materials and Design

journal homepage: www.elsevier.com/locate/matdes

On the response to hygrothermal aging of pultruded FRPs used in the civil engineering sector

Sotirios A. Grammatikos [a,b,*], Mark Evernden [a,b], John Mitchels [c], Behrouz Zafari [d], James T. Mottram [d], George C. Papanicolaou [e]

[a] BRE Centre for Innovative Construction Materials, United Kingdom
[b] Department of Architecture and Civil Engineering, University of Bath, Bath, United Kingdom
[c] Department of Chemistry, University of Bath, Bath, United Kingdom
[d] Civil Research Group, School of Engineering, University of Warwick, Coventry, United Kingdom
[e] The Composite Materials Group, Department of Mechanical Engineering and Aeronautics, University of Patras, Patras, Greece

ARTICLE INFO

Article history:
Received 28 December 2015
Received in revised form 5 February 2016
Accepted 6 February 2016
Available online 9 February 2016

Keywords:
Pultruded FRP
Hygrothermal aging
Moisture
Mechanical testing
Scanning Electron Microscopy
Computed Tomography

ABSTRACT

This paper presents the effects of hygrothermal aging on the durability of a pultruded flat sheet, immersed in distilled water at 25 °C, 40 °C, 60 °C or 80 °C for a period of 224 days. Elevated temperatures noticeably increase the moisture diffusion coefficient and moisture uptake behaviour. Measured changes in the tensile and in-plane shear mechanical properties were examined after 28, 56, 112 or 224 days. Tensile properties remained practically unaffected by aging whereas matrix dominated shear properties revealed an initial drop which was recovered to a substantial degree after further hygrothermal aging. Visco-elastic property changes due to the superimposing mechanisms of plasticization, additional cross-linking etc. were recorded. Scanning Electron Microscopy micrographs indicate that the fibre/matrix interface remained practically intact, even after the most aggressive hot/wet aging. X-ray Energy Dispersive Spectroscopy analysis showed no chemical degradation incidents on the fibre reinforcement surfaces and infrared spectroscopy revealed superficial chemical alteration in the aging matrix. Optical microscopy revealed matrix cracking in samples aged at 80 °C for 112 days. Lastly, Computed Tomography scans of un-aged material showed internal imperfections that undoubtedly enhanced moisture transport. After aging at 60 °C for 112 days, Computed Tomography detected preferentially situated water pockets.

1. Introduction

Fibre Reinforced Polymer (FRP) materials are used in engineering structures as load carrying elements as they can provide relatively high resistance to aggressive environmental conditions [1, 2]. Owing to their relative high strength and stiffness to weight ratios, and perceived enhanced durability benefits over traditional structural materials, there is growth in using FRP shapes and systems. The application of FRPs to repair and strengthen existing infrastructure is routinely practiced [3]. Exploitation of FRPs as primary and secondary structural elements [1, 2] is less developed within the civil engineering sector, and is a topic for materials and structural engineering research and development. The specific properties of FRPs [4–6] compared with structural grades of steel has activated applications in bridge deck constructions for short span highway bridges, as well as lightweight pedestrian footbridges. In many civil engineering applications, the composite processing method is pultrusion [4, 7, 8], since it is cost efficient in producing continuous lengths of constant cross-section shapes, having fibre volume fractions of 40–60%. Both mechanical fasteners and onsite adhesive bonding are used as methods of connection to fabricate primary structures from individual pultruded shapes [9]. Owing to the method of production, pultruded shapes (herein referred to as PFRP shapes) are highly orthotropic materials and their thin-walled cross-section is determined by the die's shape [10]. The direction of pultrusion is also the longitudinal direction for the PFRP shape. Often, off-the-shelf pultrudates normally have reinforcement of glass, and a matrix based on either a polyester, vinylester or polyurethane resin.

Despite service lives of 50 years or higher, civil engineering structures often lack the routine inspection and maintenance found in the aerospace and marine sectors. As a consequence, knowledge of their long-term service performance is a prerequisite for economic, safe and reliable design. Research in the field of assessment and standardization for the long-term mechanical properties of FRPs, and their structures, is therefore in high demand. A growing number of research studies is continuously being published, which can be seen as aiming to offer designers a comprehensive database for the durability performance of

* Corresponding author at: BRE Centre for Innovative Construction Materials, United Kingdom.
E-mail address: grammatikos@outlook.com (S.A. Grammatikos).

http://dx.doi.org/10.1016/j.matdes.2016.02.026

FRPs. Karbhari et al. [2] have documented the reasons that created the 'gaps' in the transfer of knowledge and technology from the aerospace to the civil engineering sector.

Moisture ingress is one of the phenomena that can adversely affect the long term durability of FRPs. The penetration of moisture penetrates from exposed surfaces induce both reversible and irreversible changes to the composite constituents [11]. Reversible changes are physical in nature, involving both property (durability) [12] and dimensional changes (swelling) [13]. Depending on the conditions and extent of hygrothermal exposure, some aging effects i.e. plasticization or softening, can be recoverable at the initial stages of aging when the absorbed water is removed and no chemical reaction occurs [14, 15]. Prolonged environmental exposure leads to irreversible changes that induce permanent property alterations within the matrix, the fibre surfaces and the fibre/matrix interface. Matrix micro-cracking [16], chain scission, residual cross-linking, hydrolysis, oxidation and plasticization are the major effects of the presence of moisture and moisture gradients [17]. The severity of the exposing conditions increases with the energy from increasing temperature.

The fibre/matrix interface and the interphase region around each individual fibre, of a few tens of nanometer thickness, are susceptible to deterioration in the presence of moisture. With adhesion between the fibres and matrix reduced due to deterioration [18], there is enhanced interfacial capillary action along the fibres that can further promote their degradation. It has been also reported that moisture attacks the fibre reinforcement leading to mechanical property loss [19]. Capillary action or 'wicking' along the fibre reinforcement has been shown to be more pronounced than moisture diffusion in the matrix of a composite, thus degrading more prominently the fibre/matrix interface rather than the matrix or/and fibres individually [20]. The latter observation is verified by the higher amount of absorbed moisture uptake in reinforced composites vs. unreinforced plain resin polymers [14, 21]. Based on that fact, moisture-induced local damage in a FRP such as hydrolysis, chain scission and permanent plasticization, is expected to be more pronounced than that in the respective plain polymer composite, due to the fundamental difference in the relative amount of total absorbed moisture [22]. All the above affect the durability of the materials and therefore modify their short and long-term performance.

Investigations towards an understanding of the long-term durability of FRPs in practical time periods can be simulated by 'short-term' accelerated aging [12, 23–33]. Accelerated aging corresponds to aging in severe conditions that provokes degradation and subsequently reduces aging time to a realistic short-term period. Additional energy applied to the system in the form of elevated temperature, increases the material's molecular mobility accelerating the chemical reactions which occur during the degradation process. However, the applicability of the accelerated aging approach depends on the material's chemical nature (chemical stability, degree of cure etc.) which may alter at high temperatures [34–36].

In a pure polymer matrix system, moisture absorption usually follows a Fickian trend [34]. Extreme environmental conditions, such as elevated temperatures and prolonged exposure times induce intrinsic chemical changes leading to deviations from the classical Fickian model [21, 35, 37]. Observed deviations can be attributed to polymer relaxation [38] and incomplete polymer curing, which ultimately allows for residual cross-linking and the leaching out of low molecular weight segments [21]. These major structural changes lead to an anomalous behaviour that impedes data interpretation and confuses the long-term prognosis. For engineering quantification the extrapolation of mechanical property variations, from aging at elevated temperatures, is typically employed to make long-term property predictions through an Arrhenius-type approach [39].

The coupling of moisture uptake with increased temperature is found to significantly influence the mechanical properties of the matrix, especially when the aging temperature approaches the Glass Transition temperature (T_g). In the early stages of aging, the presence of moisture depresses T_g by acting as a plasticizer of the matrix. Beyond a certain aging point, matrix and/or fibre/matrix interface/interphase degradation may result in leaching of low molecular weight segments. This loss of species, seen as a mass loss in the gravimetric measurements, increases the rigidity of the polymer and effects positively the T_g [12]. Leaching of non-bound substances causes an increase in T_g since non-bound segments usually act as plasticizers and subsequently their absence causes less mobility in the polymer in the longer-term [35]. Zhou and Lucas reported a similar phenomenon of T_g alterations based on un-bound and bound water molecules [15]. They reported the presence of Type-I bound water at the initial stages of aging that causes polymer plasticization and depression of T_g. After prolonged aging, the Type-II bound water leads to additional side cross-links that contribute to a T_g recovery, or a lowering in the reduction. Zhou and Lucas reported that T_g is minimum when the material moisture peaks and that T_g values are expected to elevate post-saturation [15]. Moreover, they witnessed that the higher the aging temperature the greater T_g was recovered. Interestingly, should the composite be partially cured, additional, or 'residual', cross-linking may take place, complicating further any characterization evaluation of hygrothermal aging. Additional cross-linking due to re-activation of curing, causes T_g to rise [40, 41].

The presence of moisture in polymer composites induces swelling which develops internal stresses that may instigate micro-cracking [42]. The generation of micro-cracks may increase the rate of moisture ingress and hence increase the severity of deterioration.

It is undeniable that the interference of the different mechanisms which may change when transitioning through T_g [43], may trigger fluctuations in the durability of the material which eventually may lead to negligible deterioration or even improvement of the mechanical properties [34]. The complexity of the hygrothermal aging process increases when the different mechanisms superimpose with different rates and initiation times [44].

The different possible competitive mechanisms which establish the durability during exposure are: (a) additional cross-linking due to residual curing, (b) secondary cross-linking between the polymer chains and the water molecules, (c) swelling, (d) micro-cracking, (e) leaching of low molecular weight segments (decomposition), (f) plasticization, (g) polymer relaxation etc. [1, 12, 26, 34, 45].

Fundamental works towards the understanding of the durability of FRPs have been conducted by Surathi et al. [34], Berketis et al. [46], Schutte [47], Sethi et al. [48] and Maxwell et al. [30]. Keller et al. studied the effects of natural weathering on the durability of FRPs in real service conditions [49]. In the latter, it was reported that the system and material stiffness remained unaffected after 17 years of exposure to severe Alpine environment. On the contrary Keller et al. found that the material's strength was markedly reduced, without yet influencing the structural safety of the construction [49]. The use of the Arrhenius-type protocols, such as in the proposed model from Bank et al. [39], has found a growing interest amongst those wishing to make predictions for mechanical property values in the long-term, throughout short-term hot/wet aging tests [50]. Using such protocols the durability of polymeric composites exposed to various environments has been studied in terms of the: FRP itself [26]; fibre reinforcement [51, 52]; matrix [51, 53]; fibre/matrix interface and interphase [54–56].

Despite the growing body of research in this field, the unquantified durability performance of FRPs is perceived as a major drawback hindering their wider exploitation in civil engineering structures [34]. Poor understanding of how materials change internally with in-service conditions can, undoubtedly, lead to poor designs and executions, requiring maintenance, or replacement much sooner than is desirable to achieve an acceptable level of sustainable construction [34].

This paper reports experimental findings of an extensive study concerning the effects of moisture on an 'off-the-shelf' PFRP flat-sheet material, as part of the EPSRC funded project (Providing Confidence in Durable Composites, DURACOMP, EP/K026925/1). Samples were immersed in distilled water at four different temperatures of 25 °C,

40 °C, 60 °C or 80 °C, for a period of 224 days, in accordance with the test procedure reported by Bank et al. [39]. The effects of hygrothermal exposure over time have been investigated in a test programme involving the following analyses: gravimetric; mechanical; visco-elastic (Dynamic Mechanical Thermal Analysis-DMTA), microscopic (Scanning Electron Microscopy—SEM and Optical microscopy); chemical (X-Ray Energy Dispersive Spectroscopy—EDS); tomographic (Computing Tomography—CT). The comparative study based on the evaluation of a portfolio of analysis results is used to extend the understanding on the behaviour of the changing properties of a PFRP flat sheet exposed to aggressive aqueous environments.

2. Experimental procedure

2.1. Material

The material is a five-layered glass PFRP flat sheet (FS040.101.096A) from Creative Pultrusions Inc., USA. The nominal thickness is approximately 6.4 mm. The outer surfaces of the laminate are covered by a thin protecting and non-structural polyester veil, which has the dual functions of retarding moisture ingress and protecting the PFRP from UV radiation. E-CR glass fibres serve as the reinforcement and the matrix is of an isophthalic polyester resin with unknown additives. Fig. 1 displays the structure of material comprising three Continuous Strand Mat (CSM) layers (for 2.75 mm thick) and two layers (for 3.65 mm thick) of unidirectional (UD) reinforcement. The fibre volume fractions in the two reinforcement types are 33.3% and 54.5%, respectively, giving an overall volume fraction of 45%.

All samples were cut from a single flat sheet of 2.4 m × 1.2 m using a water-cooled diamond saw. Subsequently, samples were immersed in distilled water at the four different temperatures of 25 °C, 40 °C, 60 °C or 80 °C for time periods of 28, 56, 112 or 224 days.

2.2. Testing

Sections 2.2.1–2.2.3 provide summary details regarding the tests for moisture uptake, measurement of tensile and shear mechanical properties, and of viscoelastic properties. Sections 2.2.4–2.2.6 introduce the SEM, EDS, FTIR and X-ray Computed Tomography (CT-scan) characterization methods.

2.2.1. Moisture absorption

For the moisture ingress measurements specimens were oven-dried at 30 °C for 72 h in order to remove absorbed moisture from the environment and to ensure standard initial conditioning. Square plates of 200mmx200mm and 6.4 mm thickness (h) were immersed in distilled water at 25 °C, 40 °C, 60 °C or 80 °C in thermostatically controlled Grant SUB36 water tanks. The specimen size was chosen so that it resembled real conditions with moisture absorption occurring mainly in the thickness direction. Prior to immersion specimens were weighed using a digital scale with 0.001 g sensitivity. Following immersion they were removed at pre-determined times in order to weigh the water 'uptake' in accordance with ASTM D5229. Mass ($M(\%)$) change was determined using:

$$M(\%) = \frac{M_t - M_0}{M_0} \times 100\% \quad (1)$$

where M_t is the measured mass at time t and M_o the initial dry mass. Moisture uptake measurements were conducted over a period of 224 days [39]. To calculate moisture diffusion coefficient the second Fick's law is commonly employed assuming uniform moisture and temperature conditions within the sample:

$$\frac{\partial x}{\partial t} = D\frac{\partial^2 C}{\partial x^2} \quad (2)$$

where x the is the distance in the thickness (h) direction, C is the concentration of the water and D a constant diffusion coefficient [57]. Moisture absorption and diffusion processes are functions of temperature, the type of FRP, fibre orientation and the fibre volume fraction [58, 59]. By assuming that classical Fickian diffusion takes place, D is

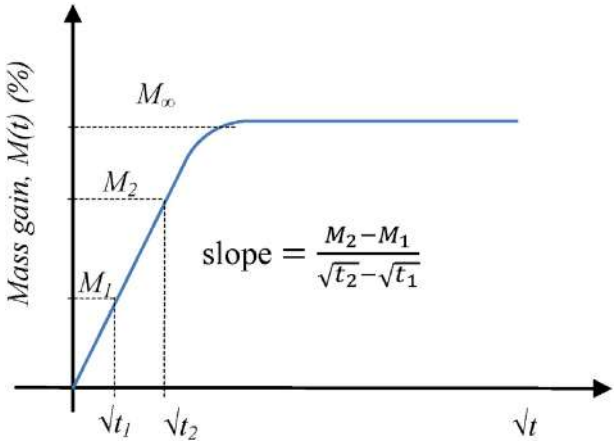

Fig. 2. Representative of a classical Fickian diffusion three-stage curve for $M(t)$ vs. $\sqrt{t}$.

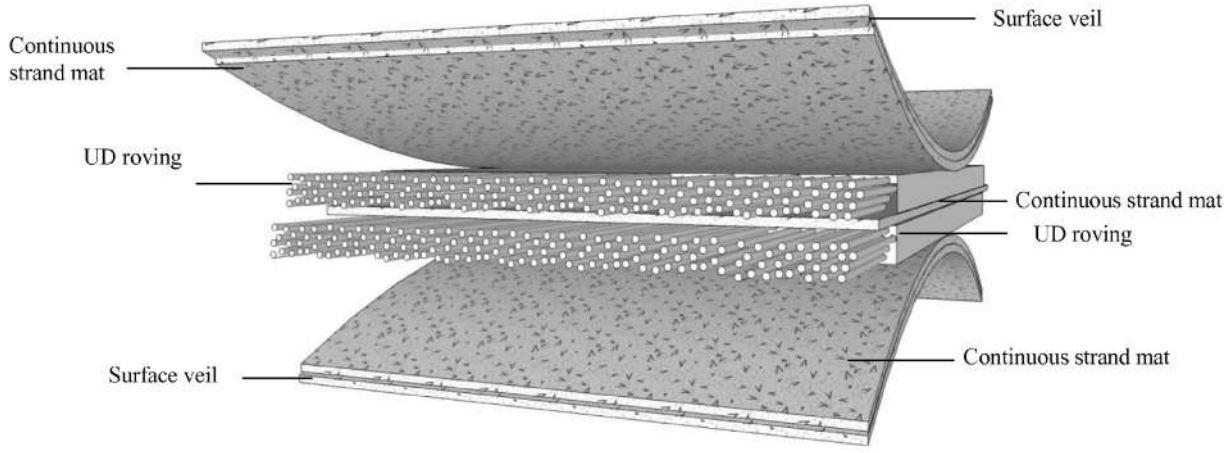

Fig. 1. Construction of 6.4 mm thick PFRP flat sheet.

calculated from the initial linear relationship of the moisture uptake with time. From the gravimetric curve shown in Fig. 2 the slope is:

$$Slope = \frac{M_2 - M_1}{\sqrt{t_2} - \sqrt{t_1}} \tag{3}$$

In Eq. (3) M_1 and M_2 are the masses of the specimen at times t_1 and t_2 obtained from the linear part of the absorption process.

The maximum absorbed moisture content is M_∞. In Fickian behaviour, D is a constant with respect to moisture concentration and temperature. According to [57] the solution of Eq. (2) for the one-dimensional approximation is:

$$\frac{M_t}{M_\infty} = 1 - \frac{8}{\pi^2}\sum_{k=0}^{\infty}\frac{1}{(2k+1)^2}\,exp\left(-\frac{D(2k+1)^2\pi^2 t}{h^2}\right). \tag{4}$$

Eq. (4) can be simplified for a short-term and a long-term approximation, as:

$$\frac{M_t}{M_\infty} = \frac{4}{\pi^2}\sqrt{\frac{Dt}{h^2}} \quad \text{for } Dt/h^2 < 0.04, \tag{5}$$

and

$$\frac{M_t}{M_\infty} = 1 - \frac{8}{\pi^2}\,exp\left(\frac{-Dt}{h^2}\pi^2\right) \quad \text{for } Dt/h^2 > 0.04. \tag{6}$$

As long as M_∞ can be established from the gravimetric curve, D for a statistical homogeneous material can be determined from:

$$D = \pi\left(\frac{h}{4M_\infty}\right)^2\left(\frac{M_2 - M_1}{\sqrt{t_2} - \sqrt{t_1}}\right)^2\left(1 + \frac{h}{l} + \frac{h}{w}\right)^{-2} \tag{7}$$

where l, w and h are for length, width and thickness of the rectilinear shaped specimen. In formulating Eq. (7) it is assumed that the moisture diffusion uptake occurs predominantly in the through-thickness direction. The final dimensional parameter in Eq. (7) accounts for the contribution in moisture absorption through the (cross-section) edges of the material [60]. Prolonged exposure can induce a deviation from this classical model and non-Fickian diffusion is observed [57, 60].

2.2.2. Mechanical testing

For the tensile coupon testing a DARTEC servo-hydraulic testing machine equipped with a 100kN load cell calibrated to BS EN ISO 7500-1 was used. To determine the strength and modulus of elasticity in the pultrusion direction, testing conducted on straight sided specimens (Fig. 3(a)) having dimensions of 250 mm × 25 mm in accordance with ISO 527-4:1997. Aluminium end tabs were bonded using Araldite 2015 epoxy adhesive in order to prevent from undesirable gripping failure during testing. Load was applied at a constant stroke rate of 2 mm/min. FLA 10-11 direct strain gauges were bonded at mid-positions on one of the 25 mm wide surfaces in order to record longitudinal strain.

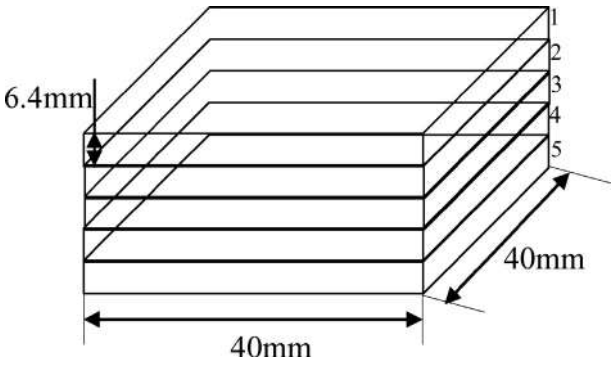

Fig. 4. Configuration of samples for the CT-scanner analysis.

To determine in-plane shear properties, both the (anticlastic) Plate-twist and Iosipescu test methods were employed. Fig. 3(b) and (c) show the test set-ups with the two different sized and shaped coupons. Loading was applied using a 50 kN capacity Instron (3369 series) testing machine that conforms to BS EN ISO 7500-1. Plate-twist tests were conducted following ISO 15310:1999, whereas Iosipescu testing according with ASTM D5379/D5379M-98. Plate-twist specimens were 230 mm × 230 mm × 6.4 mm and as shown in Fig. 3(b) the specimens were twisted using a specific rig having four loading points spaced at ~305 mm. A second specific rig was required for the Iosipescu test method, and as shown in Fig. 3(c) the specimen of 20 mm × 76 mm × 6.4 mm has two opposite-facing V-notches. In both shear tests a constant stroke rate of 1 mm/min was utilized.

For each temperature and aging time in the text matrix, batches of five or three nominally identical specimens were tested to establish the changing tensile or in-plane shear properties.

2.2.3. Dynamic mechanical thermal analysis

DMTA was used to examine and compare the visco-elastic properties between the un-aged and aged materials. Samples of the PFRP flat sheet were analyzed using a TTDMA Dynamic Mechanical Analyser (Triton technology, UK) on dual cantilever beam mode from 20 °C to 200 °C. T_g was defined by the peak of the tanδ curve.

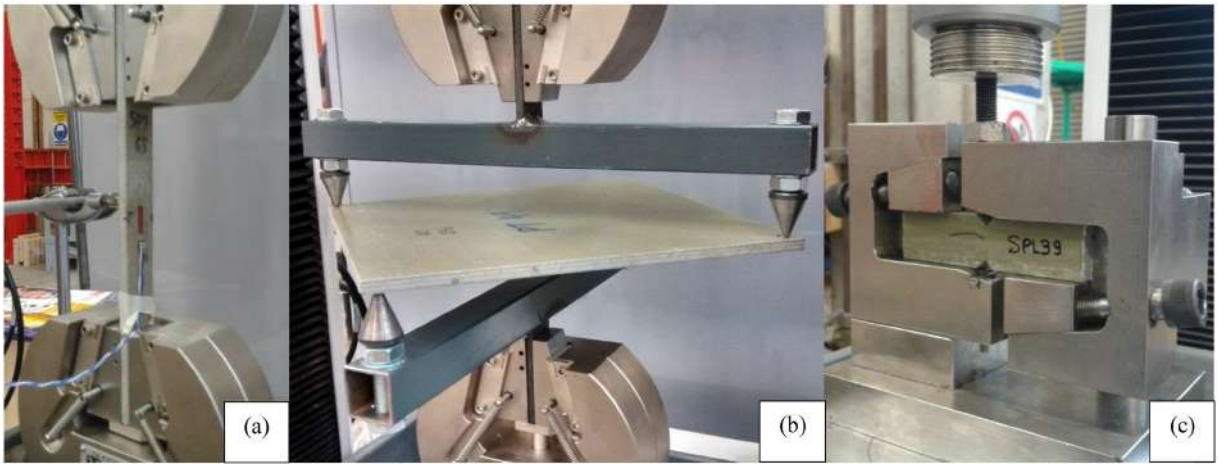

Fig. 3. Testing snapshots during: (a) tensile, (b) plate twist in-plane shear, (c) iosipescu in-plane shear.

2.2.4. Scanning Electron Microscopy

An JSM-6480LV (JEOL, Japan) SEM was employed to scrutinize the aging effects at the micro-structural level under variable pressure mode at 60 Pa to alleviate charging that would impair the imaging quality. Both un-aged and aged PFRP samples were inspected. All examined samples were metal coated with a 10 nm chromium layer to enhance the detection resolution. Captured SEM images were analyzed on a chemical basis using X-ray Energy Dispersive Spectroscopy (EDS).

2.2.5. Fourier transform infrared spectroscopy

Un-aged and aged materials were analyzed in the infrared spectra with the aim of identifying any chemical changes in the matrix due to aging. Particles of material from the bulk PFRP were collected, and for scanning, the matrix was separated from the fibres. Scans were carried out in the range of 500 cm^{-1} to 4000 cm^{-1}, using a Perkin Elmer Frontier spectrometer, equipped with a diamond MIRacle Attenuated Total Reflectance (ATR) accessory (PIKE Technologies, USA) and a Deuterated Triglycine Sulfate (DTGS) detector with KBr optics (PerkinElmer, USA).

2.2.6. Computed Tomography

The internal structure of the PFRP flat sheet was examined using a Nikon XT H 225 CT-scanner. In the case of un-aged material the tomography was employed to intrinsically identify cracks and voids. Interrogating aged samples (in their wet condition) had the objective of finding internal wet regions where the absorbed moisture had concentrated. The 'wet' samples were sealed in a plastic bag in order to prevent moisture loss during the scanning process. As illustrated in Fig. 4 five flat sheets of 40 mm × 40 mm were stacked to have a sample of ~32 mm thickness.

3. Results and discussion

In this section of the paper the test results are presented, evaluated and discussed in terms of developing an understanding of the competing mechanisms that change the mechanical properties with aging temperature and aging duration up to 224 days.

3.1. Moisture absorption

Fig. 5(a) depicts the distilled water 'uptake' curves as a function of time for immersion time to 224 days. The abscissa axis represents the $M(\%)$ using Eq. (1), while the ordinate-axis a linear scale of the soaking time in days. The solid lines indicate the gravimetric curves fitted to the experimental data. The theoretical predictions of $M(t)$ by the Fickian model Eq. (6) are given by the dashed-lined curves in Fig. 5(a). Fickian modelling was employed as a practical methodology for the determination of diffusion coefficient values. However, it was not found efficient enough in modelling the moisture uptake behaviour of the aged materials and hence, other modelling approaches such as Langmuir modelling are suggested as more appropriate [34]. It is clear for the curves that an increase in T increases the rate of moisture uptake and the maximum moisture content recorded, which after 224 days at 25 °C, 40 °C and 60 °C are ~0.98%, 1.27% and 1.82%. For the highest soaking temperature of 80 °C the maximum is 1.89% after a mere 60 days. It is worth noting that for the 25 °C soaking temperature the same specimen size absorbed almost half the amount. Furthermore, soaking at 25 °C, 40 °C and 60 °C the specimens failed to reach an equilibrium state. At 80 °C the saturation state is maintained for approximately 40 days, prior to $M(t)$ dropping to a significantly lower mass. In this context, secondary effects refer to chemical decomposition mechanisms that lead to mass loss; that was previously reported and analyzed in a recent work by Grammatikos et al. [45]. Weight changes are known to be due to: i) moisture absorption; ii) leaching out of unbound segments (decomposition); iii) leaching out of hydrolysis products (decomposition) [12, 15, 45]. The specific behaviour at 80 °C can be used to propose that the overall chemical decomposition might have been activated or, alternatively, have been more prominent after a relative short soaking period. This highlights the fact that moisture absorption and chemical decomposition mechanisms are superimposed. Moreover, it is observed that the moisture absorption process is more prominent in the initial immersion period and that chemical decomposition is most prominent in later stages, after giving a clearly identifiable peaked response in the $M(\%)$ values.

Table 1
Maximum moistures and bulk diffusion coefficients at the four aging temperatures.

Soaking temperature (°C)	25	40	60	80
D ($\times 10^{-6}$ mm^2/s)	0.42	0.52	1.15	3.26
M_∞ (%)	0.98	1.27	1.82	1.89

On the assumption that the limit of absorption is time, not temperature, dependent, it is possible that M_∞ at the three lowest temperatures can be equal or similar to that indicated and measured at 80 °C. Based on the work of Chin et al. [61] it could take several years for a composite laminate at 40 °C to attain moisture saturation. Table 1 presents the values of M_∞ and D for the material at the four constant soaking temperatures. For convenience, M_{max} is taken to be M_∞ for the specimens aged at 25 °C, 40 °C and 60 °C that had not reached equilibrium after 224 days. The values of D reported in Table 1 and Fig. 5(b) indicate that the diffusion coefficient exponentially increases with T, thereby verifying the responses plotted in Fig. 5(a).

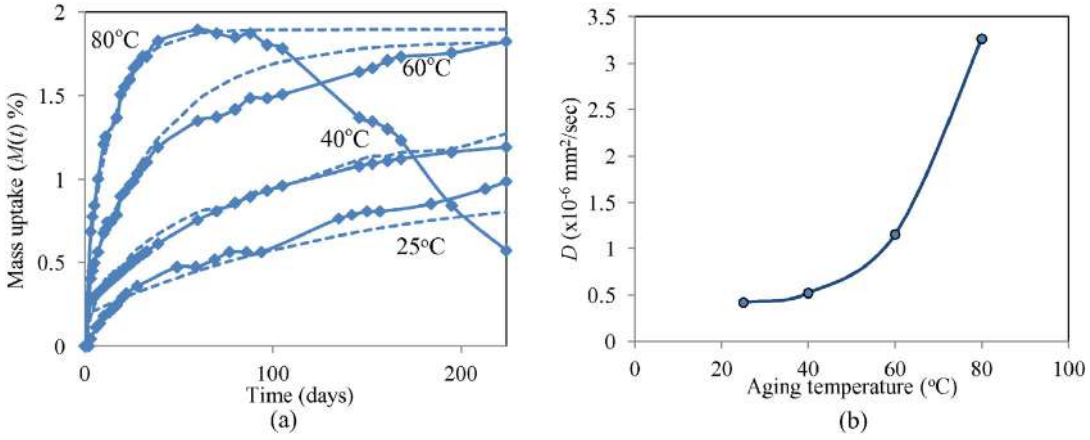

Fig. 5. (a) Moisture absorption curves with time (dashed line for calculated, continuous line for experimental), (b) diffusion coefficients.

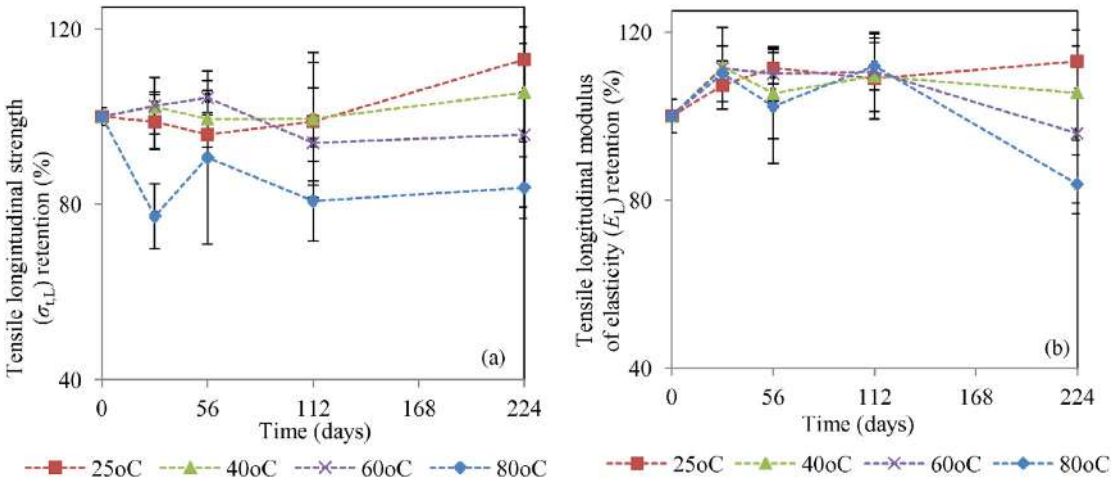

Fig. 6. Longitudinal tension with aging time and soaking temperature: (a) strength; (b) modulus of elasticity.

3.2. Mechanical testing

Mechanical testing results presented in Figs. 6 and 7 are plotted as percentage property retentions in terms of the un-aged mean measurement against time. The un-aged mean properties with range from the batch of five (tensile) or three (in-plane shear) coupons are reported in Table 2. Each plot has four different symbols that are coloured red, green, purple and blue for the constant soaking temperature of 25 °C, 40 °C, 60 °C and 80 °C, respectively. The symbols are used to position the batch means at the five testing time intervals of 0, 28, 56, 112 or 224. Error bars are used to indicate the batch variability shown in Table 2. The mean values are connected by a dashed straight line as information between these points is unknown. Fig. 6(a) and (b) present plots of the percentage property retentions for ultimate longitudinal tensile strength ($\sigma_{t,L}$) and tensile longitudinal modulus of elasticity (E_L), respectively. Equivalent changes for in-plane shear strength (τ_{LT}) and in-plane shear modulus (G_{LT}) are plotted in Fig. 7(a) and (b), respectively. As can be seen from the plots in Figs. 6 and 7 the variability in the experimental data is not constant with aging time. It is observed in Fig. 6(a) that $\sigma_{t,L}$ remains practically unaffected at 25 °C, 40 °C, and 60 °C. However, the tensile strength reduces by ~17% after 224 soaking days at 80 °C. It is observed that $\sigma_{t,L}$ exhibits an increasing tendency with time, especially at temperatures of 25 °C and 40 °C and between 112 and 224 days. Such a strength increase can be attributed to potential additional cross-linking associated with post-curing of partially-cured polyester based matrix. This strengthening effect is possibly masked by a concurrent and greater decomposition of the PFRP material at 60 °C and 80 °C. The data in Fig. 6 give an interesting finding since $\sigma_{t,L}$ exhibits a slight reduction after 56 days at 25 °C and at 40 °C, and the opposite effect at 60 °C and 80 °C. This change in $\sigma_{t,L}$ suggests a non-linear interplay of opposing mechanisms such as additional cross-linking and decomposition. At the lowest aging temperature of 25 °C a beneficial behaviour is noticeable only after 112 days. It takes only 56 days of soaking for the same outcome at the two highest temperatures of 60 °C and 80 °C. Furthermore, at 80 °C the results show a substantial degradation after only 28 days, with a recovery in $\sigma_{t,L}$ after 56 aging days, before strength is found to have lowered again at 112 days.

As seen by inspecting the results in Fig. 6(b) the retention of E_L seems to fluctuate around the un-aged value (100%) at each temperature, following an initial enhancement at 28 days. E_L is seen to remain fairly constant to 224 days at 25 °C and 40 °C. The measured longitudinal stiffness for the PFRP at 60 °C exhibits a minimal reduction after 224 days, whereas there is a 20% loss in E_L at 80 °C.

Fig. 7(a) and (b) present the τ_{LT} and G_{LT} percentage retentions with time using the Iosipescu and plate twist test methods, respectively. A characteristic trend is observed for τ_{LT} with an apparent monotonic

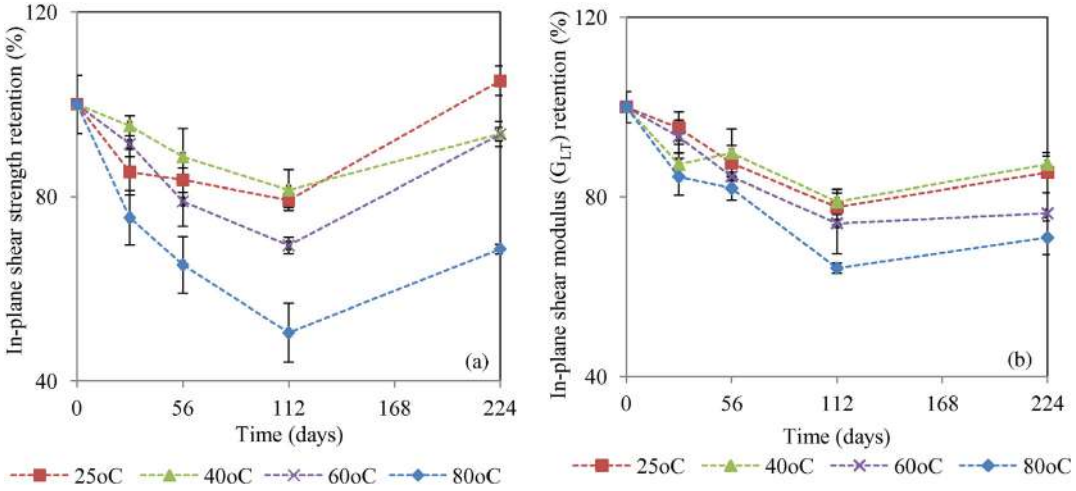

Fig. 7. In-plane shear property retention with aging time and soaking temperature: (a) strength; (b) modulus of elasticity.

Table 2
Batch longitudinal tensile and in-plane shear mechanical properties and batch glass transition temperatures.

Aging temperature	Time (days)	σ_{tL} (MPa)	E_L (GPa)	τ_{LT} (MPa)	G_{LT} (GPa)	T_g (°C)
Un-aged		389 ± 7.8	22 ± 0.9	83 ± 5.3	3.8 ± 0.1	136 ± 2.2
25 °C	28	385 ± 17	24 ± 0.2	71 ± 3.5	3.6 ± 0.1	132 ± 0.8
	56	373 ± 19	25 ± 0.9	69 ± 1.8	3.3 ± 0.1	132 ± 2.4
	112	385 ± 52	25 ± 2.4	66 ± 1.0	3.0 ± 0.1	126 ± 1.7
	224	440 ± 32	26 ± 3.1	87 ± 2.8	3.2 ± 0.1	122 ± 2.2
40 °C	28	398 ± 14	25 ± 0.3	79 ± 1.7	3.3 ± 0.1	135 ±
	56	387 ± 25	24 ± 2.5	74 ± 4.5	3.4 ± 0.2	131 ± 2.1
	112	387 ± 57	25 ± 2.5	68 ± 3.0	3.0 ± 0.1	127 ± 2.1
	224	410 ± 46	26 ± 4.4	78 ± 2.1	3.3 ± 0.1	123 ± 1.2
60 °C	28	399 ± 25	25 ± 2.4	76 ± 2.1	3.5 ± 0.1	130 ± 1.3
	56	406 ± 16	25 ± 1.6	66 ± 3.5	3.2 ± 0.1	134 ± 2.0
	112	366 ± 45	25 ± 2.3	58 ± 1.0	2.8 ± 0.2	129 ± 2.6
	224	373 ± 61	24 ± 2.9	78 ± 1.1	2.9 ± 0.3	123 ± 1.8
80 °C	28	300 ± 22	25 ± 1.6	63 ± 3.7	3.2 ± 0.1	132 ± 1.5
	56	353 ± 69	23 ± 3.1	54 ± 3.3	3.1 ± 0.1	130 ± 2.9
	112	314 ± 28	25 ± 1.4	42 ± 2.7	2.4 ± 0.1	130 ± 2.6
	224	326 ± 23	27 ± 3.1	57 ± 0.6	2.7 ± 0.1	133 ± 1.9

reduction to 112 days, followed by a significant strength recovery at 224 days. It is seen that the 25 °C and 40 °C batches at 112 days exhibited a 20% reduction in shear strength, whereas at 60 °C and 80 °C a degradation to 24% and 44% is established. Mean shear strength at 25 °C and 224 days has not only recovered completely, but improved by approximately 5% against the un-aged mean value. This indicates the possible fact that the polyester matrix had an incomplete cure after production which re-activated during hygrothermal exposure and therefore let to τ_{LT} increase. For the three other aging temperatures, the mean τ_{LT} is found to increase by approximately 12% (40 °C), 24% (60 °C) and 19% (80 °C) with aging between 112 and 224 days. Using the results for G_{LT} in Fig. 7(b) a similar trend is observed.

Due to being matrix dominated, the equivalent shear properties (Fig. 7) have been affected more than the longitudinal tensile properties (Fig. 6), which expectedly remain practically constant. The monotonic reduction in shear properties for 112 days is mainly attributed to plasticization of the polymer matrix of the composite. Nevertheless, other degrading mechanisms such as micro-cracking might have contributed to the depression of shear properties. It is worth to mention that beneficial mechanisms such as additional cross-linking might also be present, however, their effect is not likely to be distinguished unless it overcomes the potential of plasticization. In return, the final improvement in shear properties at the end of the aging regime could be attributed to additional cross-linking that occurs in the partially-cured matrix and significant leaching of low molecular weight segments. Secondary cross-links between the polymer chains and the water molecules have been also reported to occur [15]. Decomposition at this stage is present it is however being overshadowed by extensive residual curing.

3.3. Dynamic mechanical thermal analysis

Fig. 8 presents T_g changes from DMTA throughout the whole aging programme with the T_g plotted as a percentage retention of T_g for the un-aged material. The final column in Table 2 lists the T_g values of the un-aged and aged materials. The important finding is that T_g has a general decreasing trend with exposure time, which is known to correspond to plasticization and micro-cracking due to moisture-induced swelling of the bulk of polymer composite [27]. These material changes were clearly mirrored by way of the initial decreasing trend in the matrix dominated shear properties presented in Fig. 7(a) and (b). In the case of samples aged at 60 °C, it is seen that T_g was lowered from 136 ± 2.2 °C to 130 ± 1.3 °C at 28 days, before increasing by 3% at 56 days, and then reducing again to a temperature of 123 °C, which is very comparable to the T_g of PFRP material aged at 25 °C and 40 °C for 224 days. Interestingly, samples aged at 80 °C show an exponential form of reduction up to 112 days, followed by a 2% increase at 224 days. For this soaking temperature, it is believed that the degree of material degradation was insufficient to overcome the beneficial effects that might stem from additional cross-linking and the effect of leaching out of non-bound fragments. Changes in T_g are associated with changes in the chemical structure of the polyester based matrix. As mentioned in Section 1, there are different possible competitive mechanisms which dominate in the establishing of the mechanical and visco-elastic behaviour during exposure. These fundamental mechanisms interplay with each other to generate the non-linear behaviour observed experimentally supporting evaluation given in Section 3.2 for the specific characteristics of the in-plane shear properties.

Increases in moisture content have been shown to lead to increases in the magnitude and shifts to a lower temperature in loss factor curves (tanδ) [12, 62]. The drop in T_g shown in Fig. 8 may be due to the increasing presence of water within the polymer. Distribution of intermolecular chemical bonds will induce a further decrease in T_g that will affect negatively the mechanical properties. In this characterization work, it is found that storage modulus (E'), tanδ and T_g all vary according to the different structural mechanisms that control, at different times, the physicochemical and mechanical properties [12].

Fig. 9 (a to d) presents E' and tanδ vs. temperature curves for samples aged at all the investigated aging temperatures for a maximum of 224 days. The results of the un-aged material are provided by the solid line curves, and allow for a direct comparison. Changes in storage modulus are associated with the degree of additional cross-linking and decomposition while tanδ curves reveal an increasing tendency due to the presence of moisture and the extent of aging time. In Fig. 9(a), E' and tanδ of samples aged at 25 °C are illustrated. E' of samples aged for 112 and 224 days shows a drop due to the effects of significant plasticization. Samples aged at 25 °C were not expected to experience any significant cross-linking incidents owing to the lack of the necessary thermal energy to re-activate curing. Samples aged at 40 °C (Fig. 9(b)), highlighted a more complicated behaviour. There is an increase in E' (glassy region) after 28 days, followed by a decrease for the 56 and 112 days and a final recovery after 224 days. In this case the beneficial effects of cross-linking and leaching of low-molecular segments were more dominant than plasticization over the 28 days period and therefore the material was found to increase in stiffness. This behaviour was not continued for the following 112 days in which E' returned to values similar to the un-aged material. The effect of plasticization is verified by the broadening of the tanδ (Fig. 9(a) and (b)) curves with aging. This behaviour is more obvious for samples aged at 25 °C than 40 °C. Broadening of tanδ response implies higher molecular mobility

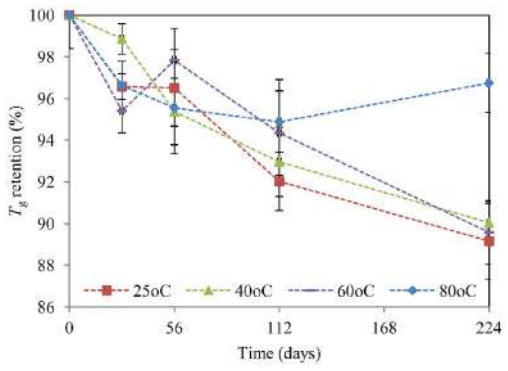

Fig. 8. Glass transition temperature (T_g) with time for the four constant aging temperatures.

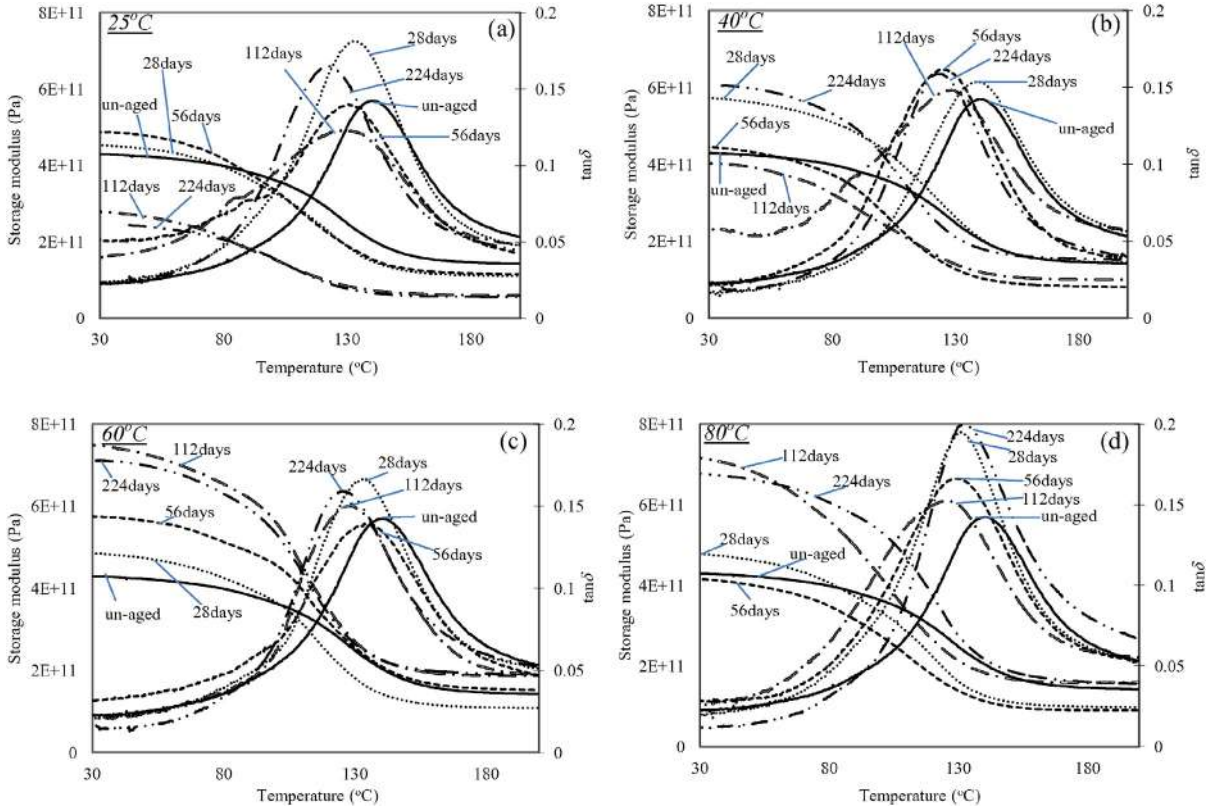

Fig. 9. Storage modulus (E') and tanδ as a function of time to 224 days and aging temperature of: a) 25 °C, b) 40 °C, c) 60 °C, d) 80 °C. Aging time curves are symbolized as follows: un-aged (-), 28 days (···), 56 days (- - -), 112 days (-··-), 224 days (-···-).

which paves the way for plasticization [12, 40, 46]. At 60 °C (Fig. 9(c)), cross-linking and leaching surpass plasticization leading to a steady increase of relative modulus. Zero or negligible broadening of the tanδ curves confirmed the masking of plasticization by opposing beneficial mechanisms. The slight increase of E' after 56 days gives confirmation to the recorded slight increase in T_g values (Fig. 8, 60 °C–56 days).

The visco-elastic behaviour of aged PFRP at 80 °C (Fig. 9(d)) was similar to that at 60 °C. It is worth mentioning that samples aged at

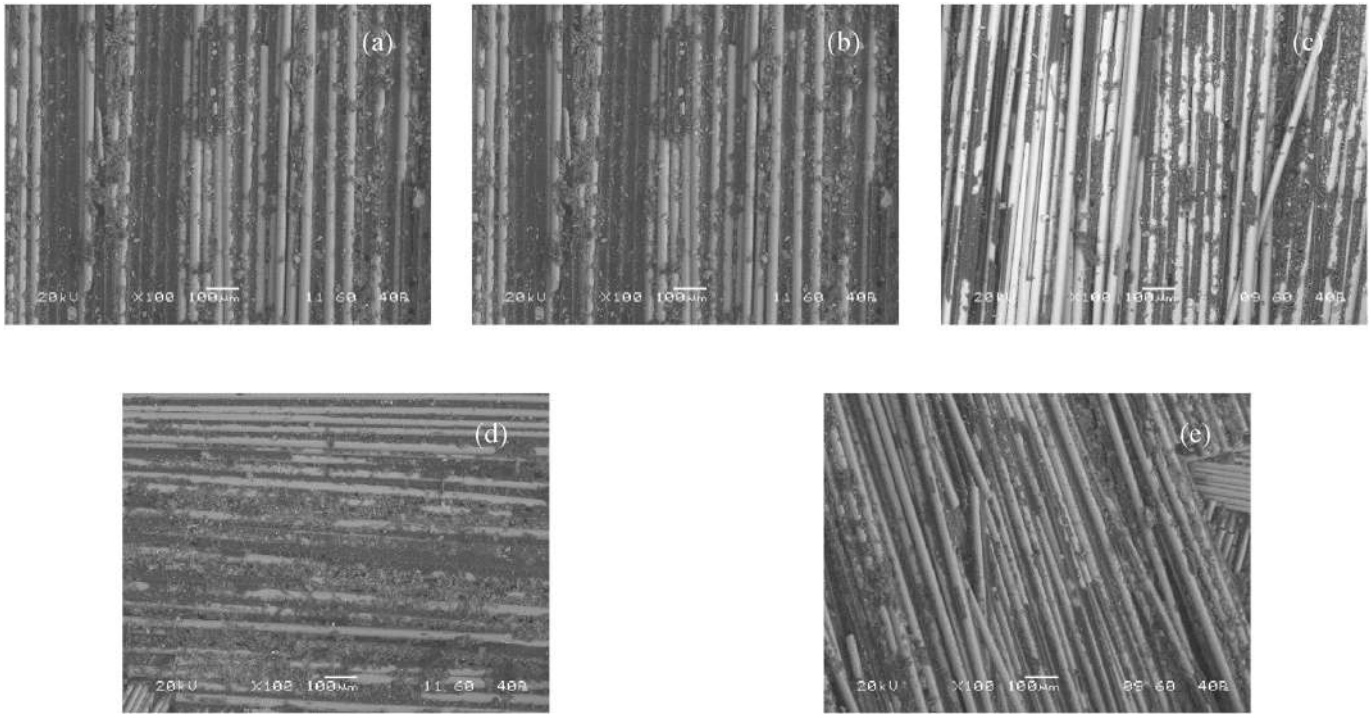

Fig. 10. SEM images of fractured surfaces: (a) un-aged; (b) 25 °C for 224 days; (c) 40 °C for 224 days; (d) 60 °C for 224 days; (e) 80 °C for 224 days.

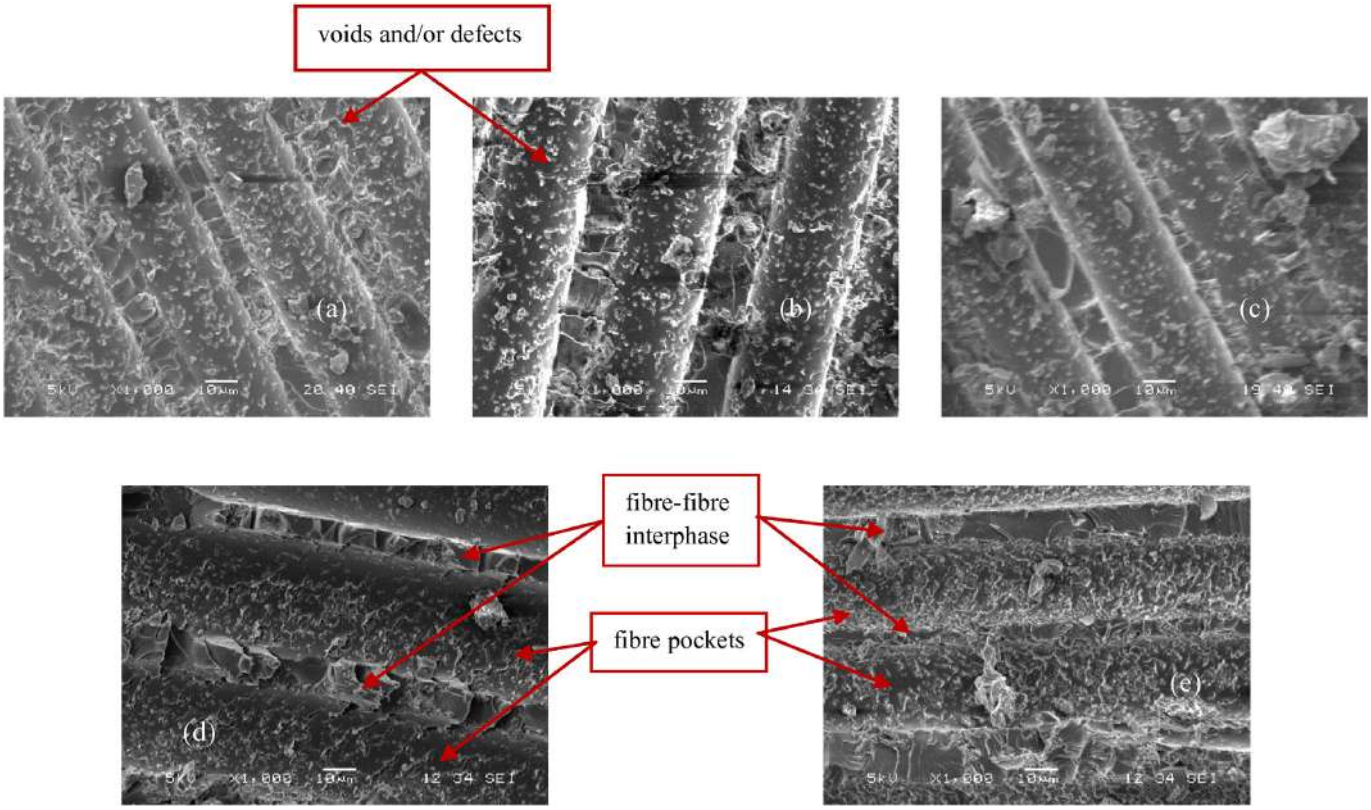

Fig. 11. SEM images of fractured surfaces showing the fibre-fibre interphase and fibre-pockets: (a) un-aged; (b) 25 °C for 224 days; (c) 40 °C for 224 days; (d) 60 °C for 224 days; (e) 80 °C for 224 days.

60 °C and 80 °C reached higher E' values as opposed to samples aged at 25 °C and 40 °C revealing the larger effect of additional cross-linking and leaching of low-molecular weight segments.

3.4. Scanning Electron Microscopy

Using the approach introduced in Section 2.2.4 SEM micrographs of fractured surfaces from failed tensile specimens are shown in Figs. 10 and 11. Images for the PFRP aged to 224 days can be compared with the un-aged material. Fig. 10 presents fractured surfaces with both matrix and fibres, whereas in Fig. 11 the higher resolution images are for the matrix only. Initial inspection finds that the fibres are firmly connected/embedded into the matrix indicating the presence of an acceptable fibre/matrix adhesion at the four aging temperatures. Closer examination of the fibre surfaces themselves in Fig. 10, shows that the majority of the fibres possess clean surfaces, suggesting a clear fibre/matrix debonding when a tensile coupon fails with the rupturing mode of failure [63].

Fractured bulk matrix surfaces were assessed using SEM with the aim of identifying any changes at the fibre/matrix interface/interphase. Fig. 11(a to e) illustrate fibre 'pockets' or matrix areas where the glass fibres had been enclosed prior to failure. The images show there to be matrix regions or fibre-fibre interphase that separate the fibre 'pockets'. Inside the pockets there are 'voids' that are not present in the fibre-fibre interphase regions. The presence of cluster-like voiding is possibly due to selectively detaching of the fibre sizing layer. Apart from the maximum accelerating aging at 80 °C, the surface texture of the pockets in Fig. 11(a) to (d) does not indicate any significant change between un-aged and aged materials for soaking temperatures of 25 °C, 40 °C and 60 °C. At 80 °C the image in Fig. 11(e) shows a rougher morphology that could be attributed to a more severe degradation of the fibre-sizing. This observation could be indicative of brittle failure or a more cross-linked interfacial bond. Overall the ten micrographs in Figs. 10 and 11 suggest that hygrothermal aging to 224 days had induced minimal changes at the micro-level and this finding supports what was discussed in Section 3.3 from an evaluation of the mechanical property test results.

The surface of the fibre reinforcement was analyzed using Energy Dispersive Spectroscopy (EDS). Table 3 reports the percentage of chemical elements present, and the totals are 100%. Comparing the five sets of results (obtained from fractured samples) and considering the variability of the technique, there is no clear trend to indicate that fibres themselves are affected by hygrothermal aging. The variation of C shown in Table 3 is attributed to the presence of residual matrix particles on the surface of the fibres.

3.5. Fourier transform infrared spectroscopy

Samples of matrix (separated from the fibres) from both un-aged and aged material were scanned in the infrared spectra. Infrared signatures of the aged PFRP (red curves) have been plotted against the un-aged spectra (blue curve) in Fig. 12, with the aim of identifying any significant chemical reactions that might have occurred during the hygrothermal aging. It is known that ester groups in polyester resins are susceptible to hydrolysis and the higher the aging temperature the more severe hydrolytic attack is expected to occur. Fig. 12(a) to

Table 3
Percent composition of chemical elements at surface of fibres at zero days and 224 days of aging.

	C	O	Mg	Al	Si	Ca
Un-aged	26.5	43.3	0.5	4.7	15.9	9.1
25 °C	20.0	43.9	0.7	5.0	20.3	10.2
40 °C	11.4	46.5	0.4	5.9	23.6	12.1
60 °C	27.6	41.3	0.4	4.8	16.9	9.0
80 °C	18.6	40.2	1.1	5.0	22.2	12.9

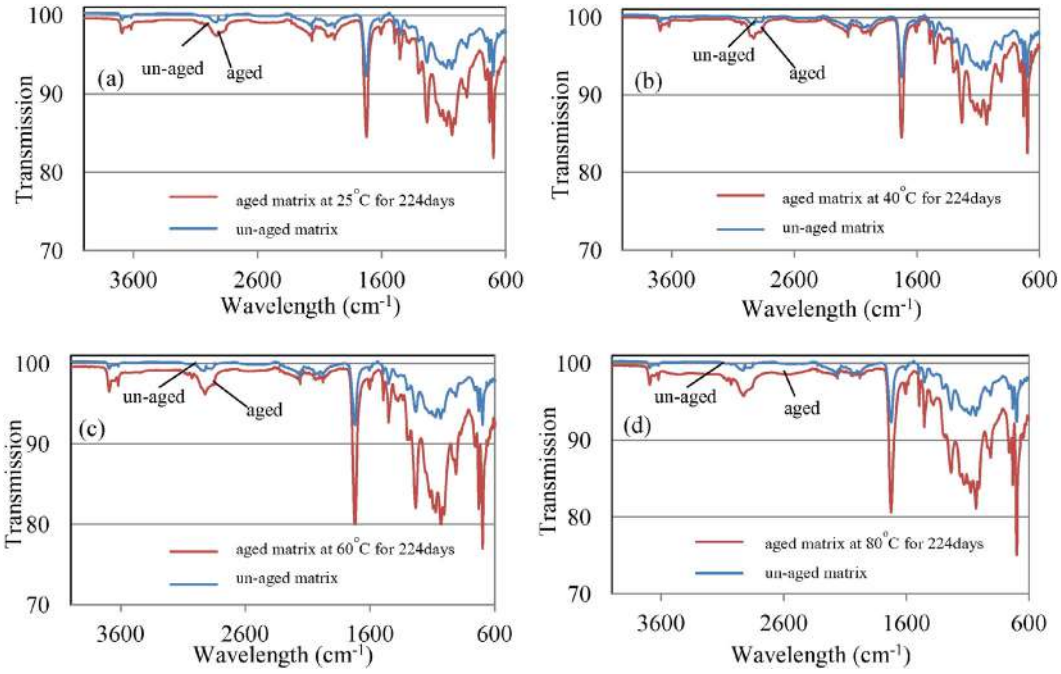

Fig. 12. Infrared spectrums of un-aged and 224 day aged matrix: (a) 25 °C; (b) 40 °C; (c) 60 °C; (d) 80 °C.

(d) present the spectra at 224 days for the four aging temperatures of 25 °C, 40 °C, 60 °C or 80 °C.

Owing to the presence of O–H there is a broad peak with weak intensity in the four parts of Fig. 12, in the wavelength region of ~3700 cm^{-1}. The next weak peak which sets at around 2960 cm^{-1} is attributed to C–H stretching. A third peak at ~1730 cm^{-1} indicates the presence of ester groups in the polyester (the carboxyl acid groups). The severity of decomposition can be determined by the maximum intensity of the O–H peak at 3700 cm^{-1} and the C–H peak at 2960 cm^{-1}. Overall, evaluation of the IR spectrums of the aged materials suggests that chemical decomposition by hydrolysis was insignificant, since, with increasing aging temperature, the change in the peaks of the O–H band is ~1% and <2% [64]. This finding from the FTIR analysis enhances the aforementioned understanding reported in Section 3.2 for the causes of the observed changes in the mechanical properties and PFRP material's microstructure.

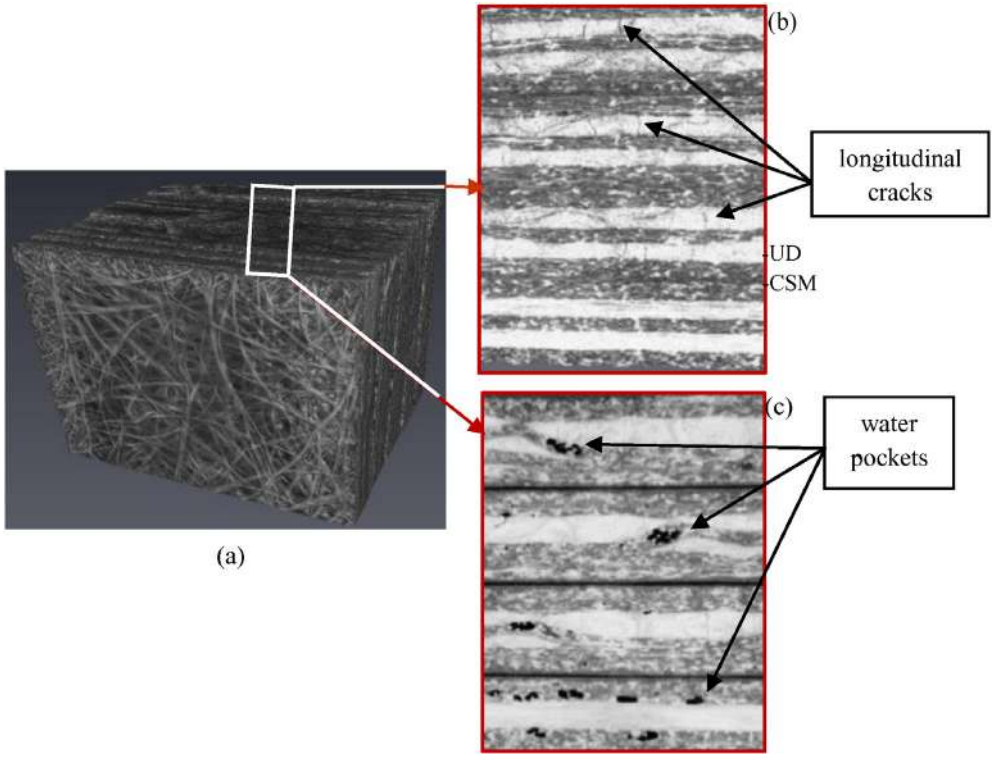

Fig. 13. CT-scanning: (a) a three-dimensional representation using a stack of five dry (un-aged) flat sheets; (b) two-dimensional image of dry (un-aged) material; (c) two-dimensional image of wet samples (aged and fully saturated).

3.6. Computed Tomography scan

Un-aged (dry) and aged (wet) samples were scanned with the aim of identifying internal imperfections and wet regions, respectively. In each case, a stack of 5 replicates was inspected for statistical purposes. Fig. 13(a) and (b) are images for an un-aged stack, whereas Fig. 13(c) is for the aged material for 112 days at 80 °C. Fig. 13(a) is a three-dimensional representation of dry material from which the structure of the front facing CSM layer is very obvious. Fig. 13(b) and (c) are images of a two-dimensional presentation through the 32 mm thickness of a stack. In these figures the direction of the continuous UD fibre layers at the bottom of the image is horizontal. Above the lowest flat sheet the rest of the sheets have their UD reinforcement direction perpendicular to that at the bottom. In Fig. 13(b) there are noticeable cracks running through the thickness of the UD layers. These cracks were potentially formed due to the relief of residual stresses developed during and after the pultrusion process and the thermal expansion mismatch between fibres and matrix. Such cracks will be responsible for a higher rate of moisture transport. Fig. 13(b) and (c) show that there are no similar cracks in the perpendicular direction using the CT-scanning imaging of the bottom flat sheet.

Fig. 13(c) presents the aged-samples (wet) case. Dark (black) areas represent water pockets mainly located within the CSM layers and at the CSM/UD layer interface. This observation suggests that the CSM/UD interface is most prone to local deterioration in the presence of moisture uptake. It may also be proposed that the longitudinal cracks formed in the UD layers appear to assist in the movement of moisture through the sheet's thickness and so the CSM layers and the CSM/UD interface act as a 'sponge' in absorbing localized concentrations of moisture.

3.7. Optical microscopy

The exposed faces (cross-sections) of samples aged for 112 days at 60 °C and 80 °C were analyzed with an optical microscope with a view to identifying the presence of surface corroding deterioration caused by hot/wet aging. The three images in Fig. 14 allow for comparison between the un-aged and aged PFRP materials. As can be seen by the 'black' areas appearing in Fig. 14(b), aging induces characteristic 'pitting' corrosion around the fibres. The severity of this phenomenon leads to cracks through the matrix, as seen in Fig. 14(c). Such matrix cracking will accelerate moisture absorption and could trigger the development of other degradation mechanisms such as delaminations, hydrolysis, fibre corrosion etc.

4. Concluding remarks

This paper presents an examination of the effects of hygrothermal aging on the durability of a pultruded E-CR glass fibre reinforced polyester matrix. Samples cut from a 6.4 mm thick flat sheet were immersed in distilled water at 25 °C, 40 °C, 60 °C and 80 °C, for a maximum aging period of 224 days. Gravimetric measurements were recorded during the whole aging regime. Changes in the tensile and in-plane shear mechanical properties were determined after 28, 56, 112 and 224 days. Physico-chemical effects were characterized by analysis using SEM, EDS, FTIR, CT-scanning and Optical microscopy. It was found that:

- Elevated temperatures accelerate the moisture absorption rate and moisture diffusion coefficient ($0.42–3.26 \times 10^{-6}$ mm^2/s). Aging at 80 °C (which is more than 40 °C below the un-aged material's T_g) revealed substantial mass loss that can be attributed to decomposition and leaching out of low-molecular weight segments into the water medium.
- Tensile strength and modulus of elasticity in the direction of pultrusion remained virtually unaffected, except for aging at 80 °C.
- Determination of in-plane shear modulus and in-plane shear strength showed that matrix dominated properties were significantly affected by hygrothermal aging. After an initial lowering, the 224 day test results showed that these mechanical properties had significantly increased compared to test results for 112 days. Changes witnessed from the mechanical testing data are believed to be due to the superimposing mechanisms of swelling, plasticization, leaching out of low-molecular weight segments and additional cross-linking.
- Dynamic mechanical analysis verified the variation of shear mechanical properties by exhibiting cross-linking, leaching and plasticization as a result of increased temperature and moisture ingress, respectively. T_g showed a continual decreasing tendency for aging to 224 days at: 25 °C (132 ± 0.8 to 122 ± 2.2 °C); 40 °C (135 ± 1.0 to 123 ± 1.2 °C); 60 °C (130 ± 1.3 to 123 ± 1.8 °C). At 80 °C, T_g (132 ± 1.5 to 133 ± 1.9 °C) was lowest at 112 days and then recovered by 3% after 224 days. This finding for the PFRP's response at 80 °C can be attributed to a greater matrix stiffness following extensive polymer cross-linking and leaching out of low-molecular weight segments.
- Scanning Electron Microscopy (SEM) micrographs indicated that the fibre/matrix interface remained practically intact after hygrothermal aging for 224 days.
- Energy Dispersive Spectroscopy (EDS) analysis showed that no significant chemical degradation occurred on the E-CR glass fibre surfaces after hygrothermal aging for 224 days.
- Infrared spectroscopy (FTIR) analysis revealed minimal chemical changes in the aged matrix. Matrix cracking, that enhances moisture ingress and subsequently accelerate aging, was detected in exposed faces (cross-section edges) of samples after aging for 112 days at 80 °C via optical microscopy.
- Computed Tomography scanning provided imaging information to locate, in un-aged material, internal imperfections in the form of cracks along the unidirectional roving bundle lengths that undoubtedly, promotes moisture transport into the body of the laminate. CT-scanning

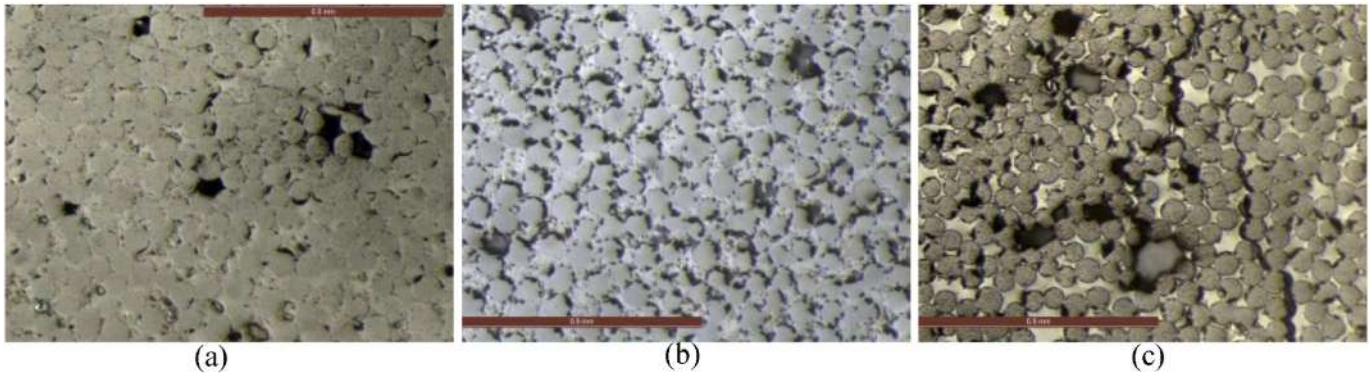

Fig. 14. Optical micrographs: (a) un-aged; (b) aged for 112 days at 60 °C; (c) aged for 112 days at 80 °C.

also detected that there were preferentially pockets of water inside samples aged at 60 °C for 112 days.

Using a standard accelerated testing protocol and combining mechanical testing with a programme of material characterization analysis methods, a qualitative understanding has been developed on the effects of competing degradation mechanisms on the durability of a commercially available pultruded flat sheet. The reported test results revealed the matrix and interface/interphase dominance on the material's response during aging.

Acknowledgments

The work is part of the EPSRC funded project DURACOMP (Providing Confidence in Durable Composites, EP/K026925/1).

References

[1] K.V. Pochiraju, G.P. Tandon, G.A. Schoeppner, Long-term Durability of Polymeric Matrix Composites, Springer, 2011.
[2] V. Karbhari, J. Chin, D. Hunston, B. Benmokrane, T. Juska, R. Morgan, et al., Durability gap analysis for fiber-reinforced polymer composites in civil infrastructure, J. Compos. Constr. 7 (2003) 238–247.
[3] I.A. Rubinsky, A. Rubinsky, An investigation into the use of fiber-glass for prestressed concrete, Mag. Concr. Res. 6 (1954).
[4] J.R. Correia, S. Cabral-Fonseca, F.A. Branco, J.G. Ferreira, M.I. Eusébio, M.P. Rodrigues, Durability of pultruded glass-fiber-reinforced polyester profiles for structural applications, Mech. Compos. Mater. 42 (2006) 325–338.
[5] V. Mara, R. Haghani, P. Harryson, Bridge decks of fibre reinforced polymer (FRP): a sustainable solution, Constr. Build. Mater. 50 (2014) 190–199.
[6] A. Zhou, L.-h. Tam, Z. Yu, D. Lau, Effect of moisture on the mechanical properties of CFRP–wood composite: an experimental and atomistic investigation, Compos. Part B 71 (2015) 63–73.
[7] B. Zafari, J.T. Mottram, Effect of hot-wet aging on the pin-bearing strength of a pultruded material with polyester matrix, J. Compos. Constr. 16 (2012) 340–352.
[8] X. Jiang, H. Kolstein, F.S.K. Bijlaard, Moisture diffusion and hygrothermal aging in pultruded fibre reinforced polymer composites of bridge decks, Mater. Des. 37 (2012) 304–312.
[9] B. Zafari, J.T. Mottram, Effect of orientation on pin-bearing strength for bolted connections in pultruded joints, Proceedings of the 6th International Conference on FRP Composites in Civil Engineering, CICE, 2012.
[10] C. Bakis, L. Bank, V. Brown, E. Cosenza, J. Davalos, J. Lesko, et al., Fiber-reinforced polymer composites for construction—state-of-the-art review, J. Compos. Constr. 6 (2002) 73–87.
[11] Environmental degradation of industrial composites, in: C.A. Mahieux (Ed.), Environmental Degradation of Industrial Composites, Elsevier Science, Oxford 2005, pp. xi–xviii.
[12] S. Cabral-Fonseca, J.R. Correia, M.P. Rodrigues, F.A. Branco, Artificial accelerated ageing of GFRP pultruded profiles made of polyester and vinylester resins: characterisation of physical–chemical and mechanical damage, Strain 48 (2012) 162–173.
[13] O. Starkova, S.T. Buschhorn, E. Mannov, K. Schulte, A. Aniskevich, Water transport in epoxy/MWCNT composites, Eur. Polym. J. 49 (2013) 2138–2148.
[14] L.V.J. Lassila, T. Nohrström, P.K. Vallittu, The influence of short-term water storage on the flexural properties of unidirectional glass fiber-reinforced composites, Biomaterials 23 (2002) 2221–2229.
[15] J. Zhou, J.P. Lucas, Hygrothermal effects of epoxy resin. Part II: variations of glass transition temperature, Polymer 40 (1999) 5513–5522.
[16] A. Hammami, N. Al-Ghuilani, Durability and environmental degradation of glass-vinylester composites, Polym. Compos. 25 (2004) 609–616.
[17] G.A. Schoeppner, G.P. Tandon, K.V. Pochiraju, Predicting thermooxidative degradation and performance of high-temperature polymer matrix composites, in: Y. Kwon, D. Allen, R. Talreja (Eds.), Multiscale Modeling and Simulation of Composite Materials and Structures, Springer, US 2008, pp. 359–462.
[18] Y. Joliff, L. Belec, M.B. Heman, J.F. Chailan, Experimental, analytical and numerical study of water diffusion in unidirectional composite materials — interphase impact, Comput. Mater. Sci. 64 (2012) 141–145.
[19] J. Hinkley, J. Connell, Resin systems and chemistry: degradation mechanisms and durability, in: K.V. Pochiraju, G.P. Tandon, G.A. Schoeppner (Eds.), Long-term Durability of Polymeric Matrix Composites, Springer, US 2012, pp. 1–37.
[20] K. Liao, C.R. Schultheisz, D.L. Hunston, Effects of environmental aging on the properties of pultruded GFRP, Compos. Part B 30 (1999) 485–493.
[21] T. Morii, T. Tanimoto, H. Hamada, Z.-i. Maekawa, T. Hirano, K. Kiyosumi, Weight changes of a randomly orientated GRP panel in hot water, Compos. Sci. Technol. 49 (1993) 209–216.
[22] T. Morii, N. Ikuta, K. Kiyosumi, H. Hamada, Weight-change analysis of the interphase in hygrothermally aged FRP: consideration of debonding, Compos. Sci. Technol. 57 (1997) 985–990.
[23] G. Carra, V. Carvelli, Ageing of pultruded glass fibre reinforced polymer composites exposed to combined environmental agents, Compos. Struct. 108 (2014) 1019–1026.
[24] Y. Wang, J. Meng, Q. Zhao, S. Qi, Accelerated ageing tests for evaluations of a durability performance of glass-fiber reinforcement polyester composites, J. Mater. Sci. Technol. 26 (2010) 572–576.
[25] A. Visco, V. Brancato, N. Campo, Degradation effects in polyester and vinyl ester resins induced by accelerated aging in seawater, J. Compos. Mater. 46 (2012) 2025–2040.
[26] J.M. Sousa, J.R. Correia, S. Cabral-Fonseca, Durability of glass fibre reinforced polymer pultruded profiles: comparison between QUV accelerated exposure and natural weathering in a Mediterranean climate, Exp. Tech. (2013).
[27] M.A. Sawpan, P.G. Holdsworth, P. Renshaw, Glass transitions of hygrothermal aged pultruded glass fibre reinforced polymer rebar by dynamic mechanical thermal analysis, Mater. Des. 42 (2012) 272–278.
[28] H.-Y. Kim, Y.-H. Park, Y.-J. You, C.-K. Moon, Short-term durability test for GFRP rods under various environmental conditions, Compos. Struct. 83 (2008) 37–47.
[29] P. Davies, G. Evrard, Accelerated ageing of polyurethanes for marine applications, Polym. Degrad. Stab. 92 (2007) 1455–1464.
[30] A.S. Maxwell, W.R. Broughton, G. Dean, G.D. Sims, Review of Accelerated Ageing Methods and Lifetime Prediction Techniques for Polymeric Materials, National Physical Laboratory, NPL, Middlesex, 2005.
[31] T.R. Gentry, L.C. Bank, A. Barkatt, L. Prian, Accelerated test methods to determine the long-term behavior of composite highway structures subject to environmental loading, J. Compos. Technol. Res. 20 (1998) 38–50.
[32] R.M. Guedes, A. Sá, H. Faria, Influence of moisture absorption on creep of GRP composite pipes, Polym. Test. 26 (2007) 595–605.
[33] R. Miranda Guedes, J.J.L. Morais, A.T. Marques, A.H. Cardon, Prediction of long-term behaviour of composite materials, Compos. Struct. 76 (2000) 183–194.
[34] P. Surathi, V.M. Karbhari, Project SSR, University of California SDDoSE, Services CDoTDoE, Hygrothermal Effects on Durability and Moisture Kinetics of Fiber-reinforced Polymer Composites, Department of Structural Engineering, University of California, San Diego, 2006.
[35] E. Boinard, R. Pethrick, J. Dalzel-Job, C. Macfarlane, Influence of resin chemistry on water uptake and environmental ageing in glass fibre reinforced composites-polyester and vinyl ester laminates, J. Mater. Sci. 35 (2000) 1931–1937.
[36] A. Apicella, C. Migliaresi, L. Nicolais, L. Iaccarino, S. Roccotelli, The water ageing of unsaturated polyester-based composites: influence of resin chemical structure, Composites 14 (1983) 387–392.
[37] Y.J. Weitsman, Anomalous fluid sorption in polymeric composites and its relation to fluid-induced damage, Compos. A: Appl. Sci. Manuf. 37 (2006) 617–623.
[38] A.R. Berens, H.B. Hopfenberg, Diffusion and relaxation in glassy polymer powders: 2. Separation of diffusion and relaxation parameters, Polymer 19 (1978) 489–496.
[39] L.C. Bank, T.R. Gentry, B.P. Thompson, J.S. Russell, A model specification for FRP composites for civil engineering structures, Constr. Build. Mater. 17 (2003) 405–437.
[40] G.C. Papanicolaou, T.V. Kosmidou, A.S. Vatalis, C.G. Delides, Water absorption mechanism and some anomalous effects on the mechanical and viscoelastic behavior of an epoxy system, J. Appl. Polym. Sci. 99 (2006) 1328–1339.
[41] P. Nogueira, C. Ramírez, A. Torres, M.J. Abad, J. Cano, J. López, et al., Effect of water sorption on the structure and mechanical properties of an epoxy resin system, J. Appl. Polym. Sci. 80 (2001) 71–80.
[42] K. Derrien, P. Gilormini, The effect of moisture-induced swelling on the absorption capacity of transversely isotropic elastic polymer–matrix composites, Int. J. Solids Struct. 46 (2009) 1547–1553.
[43] C.A. Mahieux, K.L. Reifsnider, S.W. Case, Property modeling across transition temperatures in PMC's: part I. Tensile properties, Appl. Compos. Mater. 8 (2001) 217–234.
[44] J.R. Correia, M.M. Gomes, J.M. Pires, F.A. Branco, Mechanical behaviour of pultruded glass fibre reinforced polymer composites at elevated temperature: experiments and model assessment, Compos. Struct. 98 (2013) 303–313.
[45] S.A. Grammatikos, B. Zafari, M.C. Evernden, J.T. Mottram, J.M. Mitchels, Moisture uptake characteristics of a pultruded fibre reinforced polymer flat sheet subjected to hot/wet aging, Polym. Degrad. Stab. 121 (2015) 407–419.
[46] K. Berketis, D. Tzetzis, Review on the Water Immersion and Impact Damage Effects on the Residual Compressive Strength of Composites. Resin Composites: Properties, Production and Applications, 2011 1–53.
[47] C.L. Schutte, Environmental durability of glass-fiber composites, Mater. Sci. Eng. R. Rep. 13 (1994) 265–323.
[48] S. Sethi, B.C. Ray, Environmental effects on fibre reinforced polymeric composites: evolving reasons and remarks on interfacial strength and stability, Adv. Colloid Interf. Sci. 217 (2015) 43–67.
[49] T. Keller, N. Theodorou, A. Vassilopoulos, J. de Castro, Effect of natural weathering on durability of pultruded glass fiber-reinforced Bridge and building structures, J. Compos. Constr. 20 (2015) 04015025.
[50] Springer GS, Environmental Effects on Composite Materials, 31988.
[51] L. Prian, A. Barkatt, Degradation mechanism of fiber-reinforced plastics and its implications to prediction of long-term behavior, J. Mater. Sci. 34 (1999) 3977–3989.
[52] S.P. Sonawala, R.J. Spontak, Degradation kinetics of glass-reinforced polyesters in chemical environments, J. Mater. Sci. 31 (1996) 4757–4765.
[53] M. Woo, M.R. Piggott, Water absorption of resins and composites: IV. Water transport in fiber reinforced plastics, J. Compos. Technol. Res. 10 (1988) 20–24.
[54] Y.T. Liao, A study of glass fiber–epoxy composite interfaces, Polym. Compos. 10 (1989) 424–428.
[55] L. Gautier, B. Mortaigne, V. Bellenger, Interface damage study of hydrothermally aged glass-fibre-reinforced polyester composites, Compos. Sci. Technol. 59 (1999) 2329–2337.
[56] C.J. Tsenoglou, S. Pavlidou, C.D. Papaspyrides, Evaluation of interfacial relaxation due to water absorption in fiber–polymer composites, Compos. Sci. Technol. 66 (2006) 2855–2864.
[57] J. Crank, The Mathematics of Diffusion, Clarendon Press, 1975.

[58] R.M.V.G.K. Rao, N. Balasubramanian, M. Chanda, Factors affecting moisture absorption in polymer composites part I: influence of internal factors, J. Reinf. Plast. Compos. 3 (1984) 232–245.
[59] R.M.V.G.K. Rao, M. Chanda, N. Balasubramanian, Factors affecting moisture absorption in polymer composites part II: influence of external factors, J. Reinf. Plast. Compos. 3 (1984) 246–253.
[60] C.-H. Shen, G.S. Springer, Moisture absorption and desorption of composite materials, J. Compos. Mater. 10 (1976) 2–20.
[61] J.W. Chin, K. Aouadi, M.R. Haight, W.L. Hughes, T. Nguyen, Effects of water, salt solution and simulated concrete pore solution on the properties of composite matrix resins used in civil engineering applications, Polym. Compos. 22 (2001) 282–297.
[62] I. Ghorbel, D. Valentin, Hydrothermal effects on the physico-chemical properties of pure and glass fiber reinforced polyester and vinylester resins, Polym. Compos. 14 (1993) 324–334.
[63] R. Felipe, R. Felipe, E. Aquino, Laminar composite structures: Study of environmental aging effects on structural integrity, J. Reinf. Plast. Compos. 31 (2012) 1455–1466.
[64] M.A. Sawpan, A.A. Mamun, P.G. Holdsworth, Long term durability of pultruded polymer composite rebar in concrete environment, Mater. Des. 57 (2014) 616–624.